Material Transport by
eanography. **31**, 275-

ted to water exchange

c/Anoxic Interface by

istry of the Black Sea

CIRCULATION AND HYDROGRAPHIC CHARACTERISTICS OF THE BLACK SEA DURING JULY 1992

TEMEL OGUZ
Middle East Technical University, Institute of Marine Sciences, Erdemli, Icel, TURKEY
L. I. IVANOV
Marine Hydrophysical Institute, Ukranian Academy of Sciences Sevastopol, UKRAINE
SÜKRÜ BESIKTEPE
Middle East Technical University, Institute of Marine Sciences, Erdemli, Icel, TURKEY

Abstract: Hydrographic measurements performed during July 1992 are used to infer sub-basin and mesoscale circulation and water mass characteristics of the Black Sea. A notable feature of the circulation is the convoluted cyclonic boundary current system with distinctly different T, S characteristics. The coastal side of the Rim Current is characterized by a series of mesoscale eddies. The interior has a weaker circulation and little marked structure within an elongated low pressure cell. The baroclinic geostrophic flow field is vertically coherent and possesses smaller amplitude meanders as compared with the previous September 1991 observation (Oguz et al.,1994). In the northwestern shelf region, the fresh water inflows from the Danube as well as Dniepr and Dniestr Rivers give rise to a strong coastal salinity front confined above the seasonal thermocline. Both the coastal current and the Rim Current exhibit strong onshore-offshore meanders, indicating significant interaction between the interior and northwestern shelf waters. The influence of the fresh water inflow can be traced up to the east of the Bosphorus exit region, ~32 °E. The anoxic interface, identified by the 16.2 sigma-t surface, is located at levels deeper than 150 m along the coast, but is elevated sharply across the Rim

L.I. Ivanov and T. Oguz (eds.), Ecosystem Modeling as a Management Tool for the Black Sea, Vol. 2, 69-91.

Current frontal zone to its shallowest position of about 100m within the interior cyclonic cell.

1. Introduction

Severe environmental problems in the Black Sea brought scientific institutions from the riparian countries together to carry out coordinated interdisciplinary oceanographic studies. Following several multi-institutional, joint efforts performed during the late 1980's (e.g. R.V. Knorr cruises in 1988; Murray, 1991) and in September 1990 (Oguz et al., 1993a), the first complete coverage of the sea with approximately 20 miles station network was realized during September-October 1991 (HydroBlack'91). The pooled and intercalibrated data obtained in this basinwide multi-disciplinary, quasi-synoptic survey provided detailed spatial distribution of important physical and biochemical parameters and their interrelations with the mesoscale features (Tugrul et al., 1992; Saydam et al., 1993; Oguz et al., 1994; Basturk et al.,1994). The second basinwide survey with a similar station network was conducted during July 1992. In the following years, field efforts (e.g. April 1993, August 1993, May 1994, March 1995, July 1996) were devoted more to regional scale process-oriented investigations.

When the results of these recent surveys are compared with the climatological studies (e.g. Blatov et al., 1984; Eremeev et al., 1992), the emerging picture of the general circulation is not simple as it was thought to be historically. The results (e.g. Oguz et al., 1993a, 1994) show considerable complexity within the upper and intermediate levels with mesoscale features dominating the general circulation in the basin. The larger scale, quasi-persistent features of the circulation involve a narrow jet-like boundary flow around the basin, and various subbasin scale features and large mesoscale eddies on both sides of the peripheral current. The flow system appears to be complicated further through interactions among and instabilities of the large scale flow structures by giving rise to the features such as fronts, time dependent and rapidly evolving meanders, offshore jets and mesoscale eddies. Various forms of such mesoscale features are described by satellite images in Oguz, La Violette and Unluata (1992) and Sur, Ozsoy and Unluata (1994). These features are further supported by the eddy resolving numerical modeling studies by Oguz et al. (1995), Oguz and Malanotte-Rizzoli (1996), Stanev et al. (1995), Rachev and Stanev (1997).

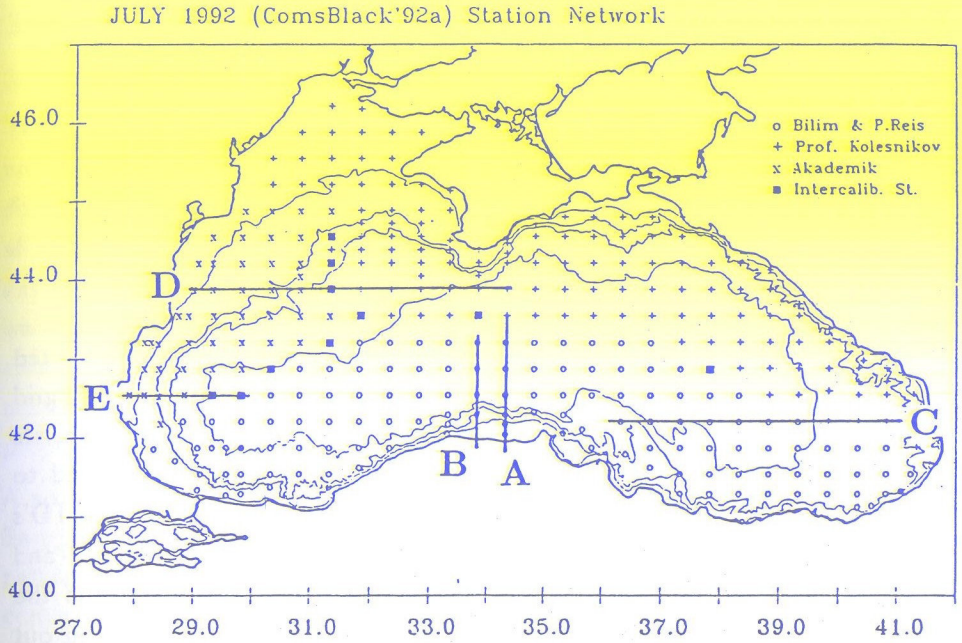

Figure 1. Station network and bathymetry of the Black Sea with sections referred to in the text. The bathymetry includes only 200, 1000 and 2000m contours

One of the objectives of the July 1992 field survey was to elaborate further the horizontal and vertical structures of the general circulation in terms of its variabilities, processes and interactions on a variety of scales and to provide an additional basis for carrying out regional process oriented studies, interdisciplinary ocean science operational and management applications. The present work describes the circulation and thermohaline characteristics obtained from this survey. The major physical and biochemical characteristics of the northwestern shelf region was presented before by Aubrey et al. (1996) and complement the present study. The paper is organized as follows. The data acquisition and analyses are described in Section 2. The results are presented in Sections 3 and 4, followed by a summary and conclusions in Section 5.

Table 1. Cruise inventory for the July 1992 Survey

Vessel	Country	Dates	No. of Stations
R.V. Akademik	Bulgaria	7-17 July	55
R.V. Bilim	Turkey	4-26 July	135
R.V. Koloesnikov	Ukraine	7 July- 2 August	138
R.V. K.Piri Reis	Turkey	4-18 July	66

2. Data

The data presented in this paper are based on the CTD measurements collected quasi-synoptically by four ships during July 1992 (Table 1). The sampling grid (Fig. 1) is the same as the one used in the HydroBlack'91 survey and consists of more than 300 stations with the nominal spacing of 20 miles, reduced to about 10 miles or less at some regions of interest. The SeaBird-SBE9 CTD's are used in the Turkish ships R.V's Bilim and K.Piri Reis whereas Istok-7 and Istok-5 are used on board the Ukranian ship R.V Prof. Kolesnikov and the Bulgarian ship R.V Akademik, respectively. The CTD casts were carried out to the nominal depth of 500 dbar, except at the intercalibration stations where the full depth was covered. The data, consisting of vertical profiles of the temperature and conductivity at one dbar intervals, were intercalibrated and pooled together. The pooled data set was then used to obtain salinity, potential temperature and potential density and dynamic height. The final data set is accurate to about 0.005 °C in the temperature and 0.005 in the salinity. The details of the intercalibration and data processing procedures are presented in Oguz et al. (1993b).

A shipborne Acoustic Doppler Current Profiler (ADCP) with a 150 kHz transducer was operated continuously on the R.V Bilim in the southern part of the sea within the Turkish exclusive economical zone. Vertical profiles of the eastward and northward current components were obtained along the ship track to a maximum depth of 350 m. The ADCP was configured to alternate "water track" or "bottom track" pulses, depending on the depth of the bottom topography, with a pulse length of 8 m, a vertical bin length of 4 m, and an ensemble averaging period of 15 minutes. Because of malfunctioning of the GPS receiving system of the ship during the survey, the absolute current velocity components were obtained only relatively with respect to those in the 262-286 m depth band. The velocity data were converted to geographic coordinates using the satellite navigation and gyro systems of the ship.

3. Circulation Characteristics

3.1. GEOSTROPHIC CURRENT FIELD

The baroclinic flow structure is described in Fig. 2 by means of the dynamic height topography (DHT) maps at selected pressure levels with respect to 500 dbar reference level. Our experience from the other studies (e.g. Oguz et al.,1993a, 1994) indicates that this choice of the reference level adequately describes the features of the upper layer circulation. As in Oguz et al. (1994), we present the dynamic height fields and other property distributions by hand-contoured maps since the optimally-estimated maps smooth the fields and thus are unable to resolve mesoscale variability of the circulation and water mass properties.

A notable feature of the DHT maps presented at 4, 100, 250 dbar levels (Fig's. 2a-c) is the vertical coherency of the flow field with depth. The circulation pattern consists of a cyclonic boundary flow of the Rim Current over the steep continental slope of the Black Sea. It is flanked on its interior side by an elongated cyclonic cell. At the 4 dbar level (Fig. 2a), the cyclonic cell includes two distinct zonally elongated gyres separated from each other within the central part of the sea by meanders of the Rim Current from both sides. The eastern gyre is compressed along the east-west direction towards the northern flank of the Rim Current, whereas the southern part of the eastern-central basin is identified by a very weak (almost motionless) current system. At deeper levels, the western cyclonic gyre preserves its identity while the eastern gyre is characterized by several mesoscale eddies (Fig. 2c). Onshore of the Rim Current constitutes a narrow coastal zone of the anticyclonically-dominated flow with a series of distinct eddies, most of which have been identified in the earlier surveys (Oguz et al., 1993a,1994). Once again, the Batumi Eddy emerges as the largest anticyclonic feature occupying the southeastern corner of the basin.

Most pronounced meandering of the Rim current occurs over the relatively wide topographic slope region connecting the northwestern shelf area to the interior of the western basin. In the rest of the basin, the Rim Current possesses small amplitude (20-30 km) meanders with a spatial periodicity of about 100-150 km at all depths. At sub-pycnocline levels, more pronounced meanders

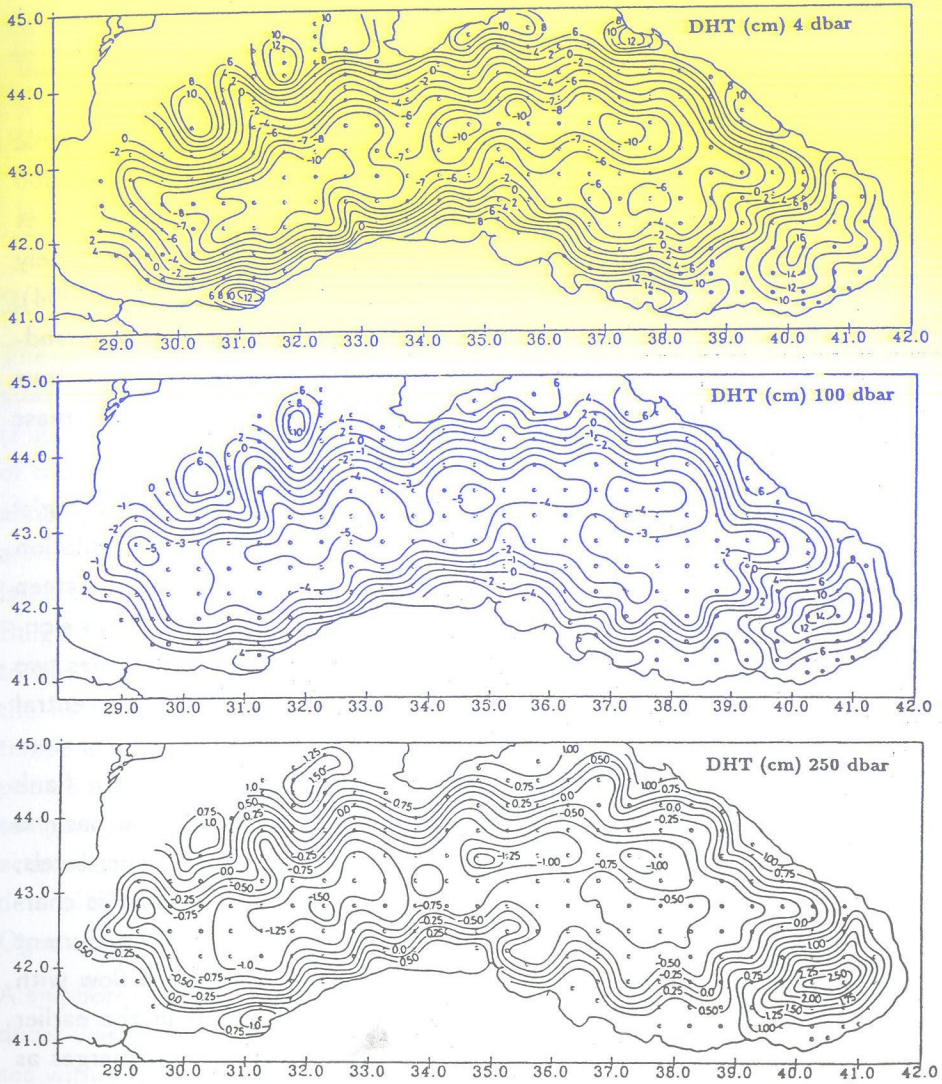

Figure 2. Dynamic height topography maps (cm) relative to 500 m depth at (a) 4 m, (b) 100 m, (c) 250 m. The contour intervals vary for clarity of presentation.

exist along the soutern coast between approximately 35 and 38°E longitudes (Fig. 2c), associated with the topographic rectification of the flow due to the canyon-ridge structure (see Oguz et al., 1991 for the details of the regional topography). This local topographic controll is, however, not dominant above the sharp permanent pycnocline acting as the boundary for the upper layer circulation.

Off Cape Sinop, near 35°E longitude, the Rim Current splits into two branches near the surface. Its main part deflects towards southeast and follows the Turkish coast with a core speed of about 30 cm/s. The inner part proceeds eastward forming a mid-basin current as a part of the elongated of the eastern basin. The area within the interior of the eastern basin, surrounded by the Rim Current on the south and the cyclonic gyre on the north, is a relatively quiescent region within the upper layer (Fig. 2a,b) and identified by an anticyclonic eddy at the sub-pycnocline levels (Fig. 2c). Phytoplankton bloom event was recorded in this region during the time of measurements (Yilmaz et al., 1998). The secchi disk depths were about only 2-4 m (Vladimirov et al., 1997), and the light transmission not more than 50% within the surface layer above the seasonal thermocline. The peculiar chemical characteristics of the region was described by Konovalov et al. (1997).

The baroclinic currents decrease with depth slowly in the upper 150 m, and more rapidly below. The maximum surface geostrophic current speed is about 35 cm/s observed along the main axis of the Rim Current (Fig. 3a). It decreases to 20 cm/s at 100 m depth and 5 cm/s at 250 m depth with apparent horizontal shears at all levels. The currents are considerably weaker within the interior as compared with the Rim Current zone. The 4 dbar relative vorticity field (Fig. 3b) reveals clearly the anticyclonically dominated coastal zone separated by a lateral shear zone from the cyclonic cell of the basin's interior.

The optimally-mapped surface geostrophic current pattern given in Fig. 3a is similar to that of September 1991 survey (see Fig. 4c in Oguz et al. 1994) except few details on the Rim current structure and the interior of the cyclonic cell. The hand-contoured dynamic topography maps however reveal several important differences in the mesoscale structure of the flow. While Fig. 4a of the September 1991 survey in Oguz et al. (1994) yields a series of offshore filaments and large meanders along the periphery, the present survey possesses only small amplitude meanders although wavelength of the meanders varies between 100 to 150 km in both surveys.

4 dbar geostrophic currents

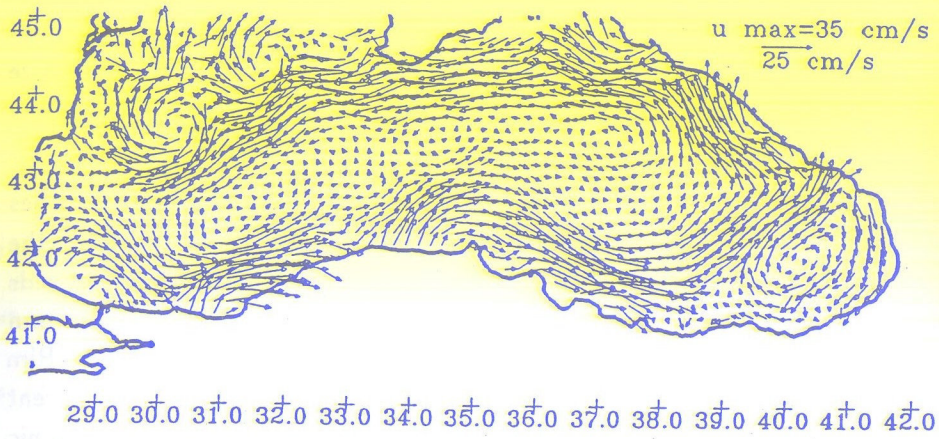

Figure 3a. Geostrophic current field (cm/sec) at 4 m depth computed from the optimally-mapped dynamic height field.

rel. vorticity 4 dbar

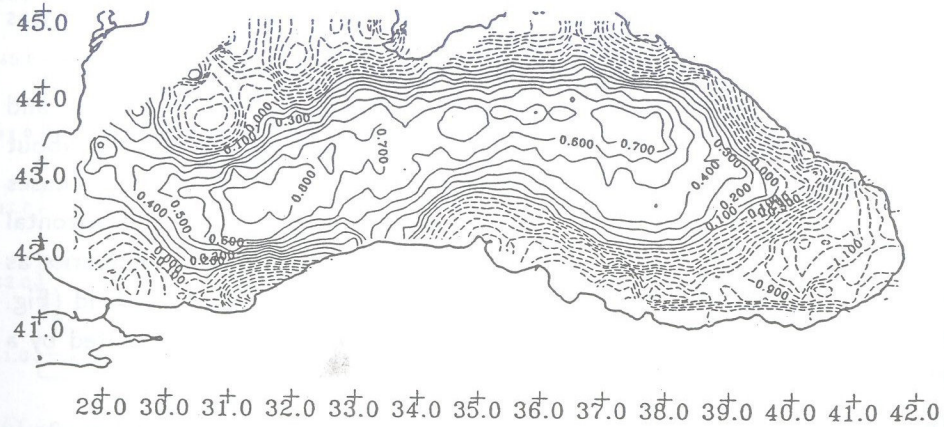

Figure 3b. Relative vorticity field (sec^{-1}) at 4 m depth computed from the optimally-mapped dynamic height field. The solid (broken) lines define the regions with cyclonic (anticyclonic) vorticity.

3.2. ADCP CURRENTS

The ADCP currents measured along the ship track of the R.V Bilim yield qualitatively a consistent picture of the flow field with those obtained from the dynamic height computations. Quantitatively, the ADCP measurements reveal stronger currents up to a maximum difference of 20 cm/s near the surface. Fig. 4a, displaying the ADCP current distribution at 20 m depth, indicates the strongest currents of 50 cm/s along the main axis of the Rim Current. The southeasterly flow outside the Bosphorus exit region, as well as three meanders along the Turkish coast between 31°E and 35°E longitudes are the most notable features common for these two different current patterns. The large cyclonic eddy within the interior of the western basin as well as the anticyclonic eddy of the eastern basin interior are also traced in Fig. 4a. The Batumi anticyclonic gyre is captured only partially in the ADCP measurements near the eastern end of the sea.

The details of the vertical and cross-stream structure of the Rim Current obtained by the ADCP measurements are presented in Fig. 4b along the meridional section at 34°45'E (section A in Fig. 1), near Cape Sinop. Both eastward and northward components reveal vertical uniformity of the boundary current system within the upper 75 m, followed by a considerable shear zone up to 125 m depth. The typical vertical shear, on the order of ($0.25\ ms^{-1}/50m$)=$0.05\ sec^{-1}$, takes place across the permanent pycnocline. The core of the jet has a width of about 30 km and is characterized by currents of 50 cm/s within the upper uniform layer. The jet core is separated from the coast by a narrow anticyclonic shear zone. On its offshore side, the jet is connected to the interior circulation by a smoother transition zone with cyclonic shear of the order of ($0.2ms^{-1}/40km$).

4. Hydrographic Characteristics

The quasi-synoptic map of the surface temperature field (Fig. 5a) shows considerable spatial inhomogeneity in response to the changing meteorological conditions during the cruise. It varies between the two extreme values of 26 °C and 14 °C in the basin. The coldest patch of water is centered at 34°E longi-

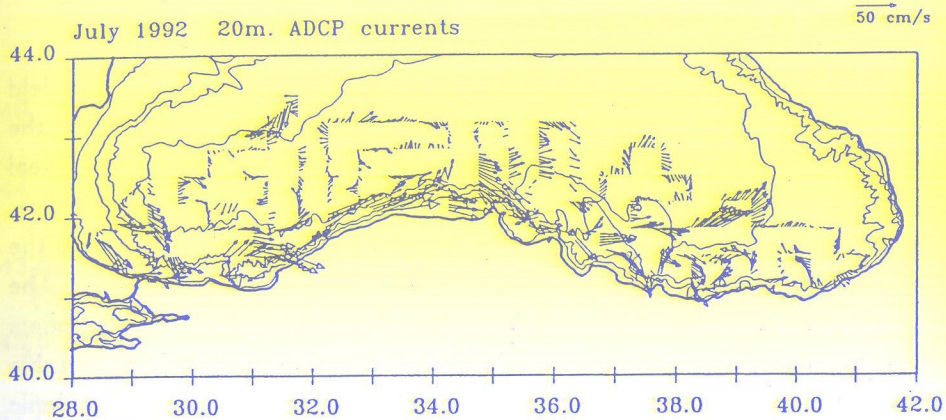

Figure 4a. ADCP currents (cm/sec) at 20 m depth measured along the ship track of the R.V. Bilim in the southern Black Sea.

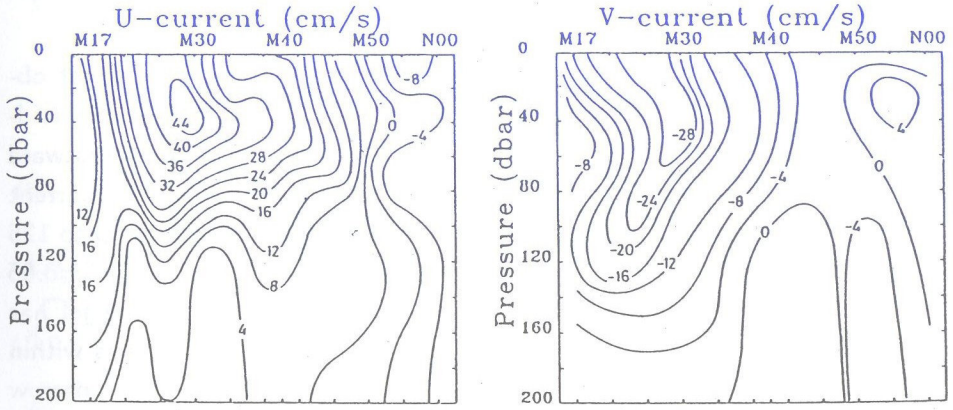

Figure 4b. Eastward and northward components of the ADCP currents (cm/sec) along the meridional section A, near the Cape Sinop.

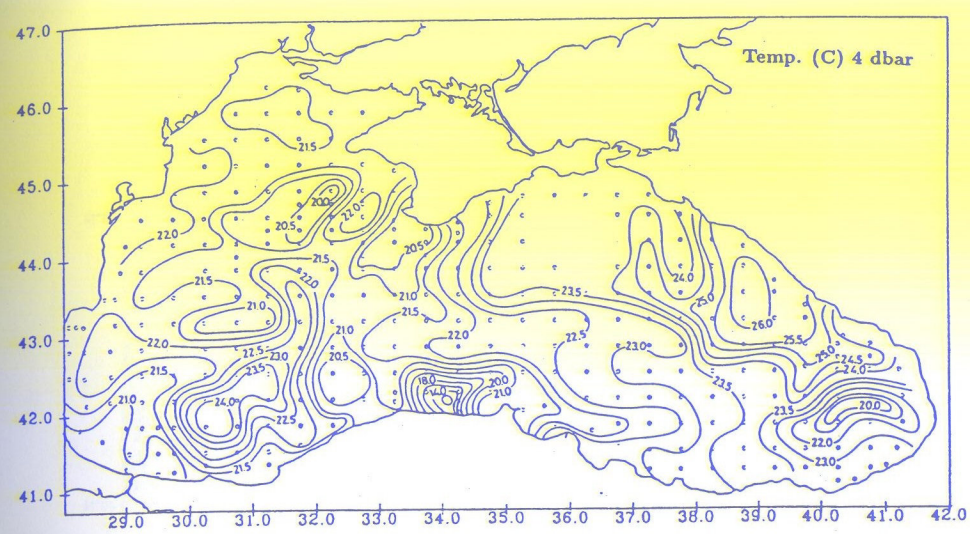

Figure 5a. Potential temperature distribution (°C) at 4 m depth. The contour intervals vary for clarity of presentation.

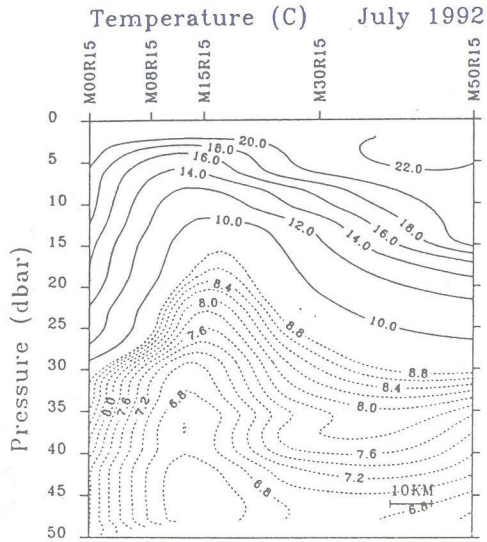

Figure 5b. Meridinal temperature transect off the Turkish coast, along the section A shown in Figure 1.

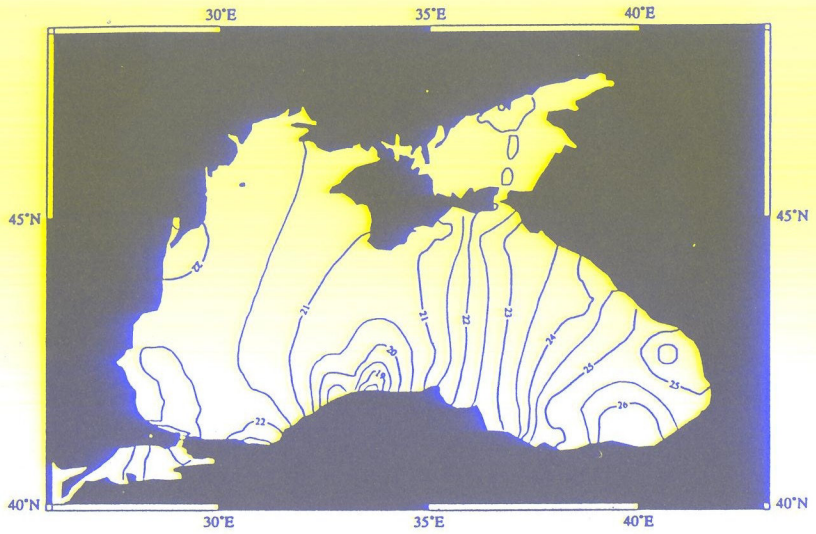

Figure 5c. Sea surface temperature pattern (degrees C) derived from a composite AVHRR imagery for 9-to-15 July 1992.

tude along the Turkish coast, extending further west to 32°E. This anomalous feature is associated with the coastal upwelling phenomenon in response to the strong northeasterly winds affecting the western and central basins from July 10 to July 12. The presence of this cold water patch is shown by the meridional temperature cross-section (section B in Fig. 1) in Fig. 5b and can also be traced in the weekly-averaged (9-to-15 July 1992) satellite-derived SST map (Fig. 5c). The meridional temperature front at 32°E along the Turkish coast marks the measurements on board R.V Bilim before and after the storm event. The effect of the upwelling-induced winds on the surface waters of the western-northwestern shelf region is also evident in Fig. 5a by relatively cooler temperatures of the region. As shown in Table I, the hydrographic measurements performed in this region by the R.V Akademik coincide with the period of upwelling favorable wind event.

A cold water spot is also observed near the southeastern end of the basin one week later in response to the passage of this low pressure center over the Black Sea. The temperature decrease at the surface in the southern part of the eastern basin within this one week period after 15 July 1992 can be seen by comparision of Fig. 5a with Fig. 5c. As shown for section C in Fig. 5d,

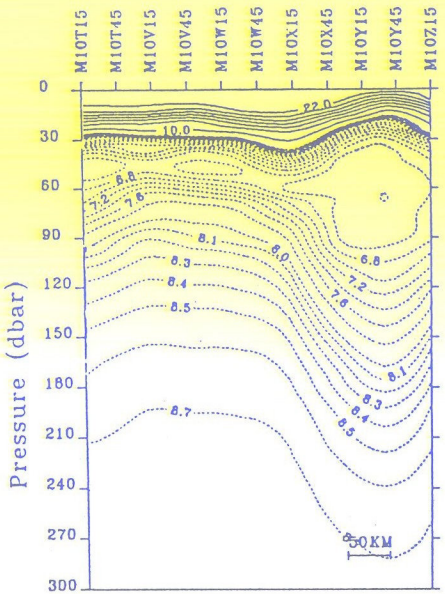

Figure 5d. zonal temperature transect along the section C shown in Fig. 1 within the eastern basin.

we note that the cold water spot near the southeastern part of the sea is the surface intensified feature, confined only above the seasonal thermocline. At deeper levels of the upper layer, the temperature transect reveals downwelling structure consistent with the permanent anticyclonic character of the region. The cyclonic circulation which should be associated with the transient response of the upwelling does not, however, appear in the surface dynamic height anomaly map.

A distinguishing feature of the surface salinity distribution (Fig. 6) is the pronounced onshore-offshore salinity variations throughout the basin. The most pronounced variations take place along the western coast due to the fresh water inflow from River Danube as well as Dniepr and Dniestr. The brackish coastal water is traced along the coast on both sides of the Danube estuary. To its north, the salinity of the coastal waters are about 16.0. Considering the fact that the inflow from Dniepr and Dniestr is much lower (less than one third of the Danube), the northward deflection of the part of the Danube inflow (confirmed by the numerical model in Oguz et al.,1995 as well as satellite imagery) may also contribute to the formation of such low salinity zone along the northwestern coast. To the south, the low salinity waters extend up to the

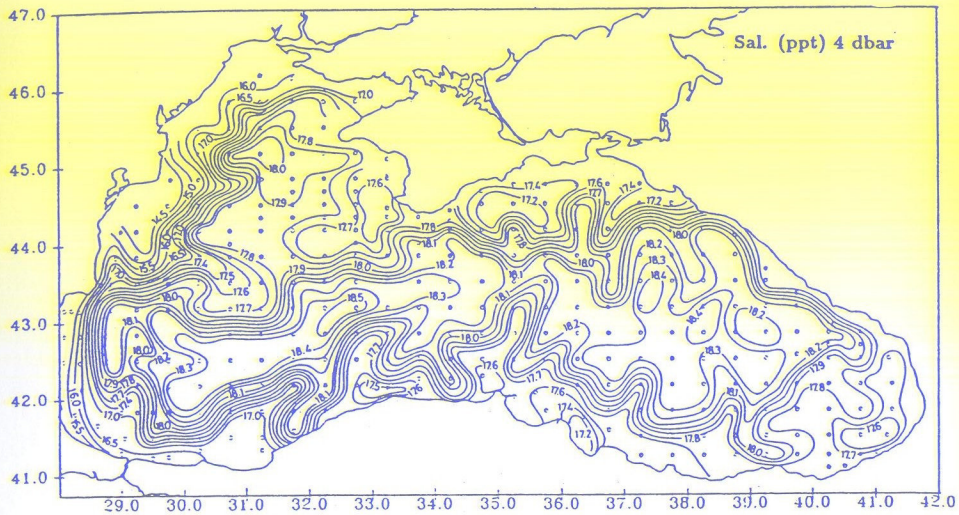

Figure 6. Salinity distribution at 4 m depth. The contour intervals vary for clarity of presentation.

Bosphorus entrance region in the form of a narrow coastal strip of current with salinities greater than 15.5. The lowest salinities of about 14.5 are present to the south of the Danube estuary.

At the surface, the fresh water coastal zone is separated from the rest of the northwestern shelf by an inner-shelf front which has a typical width of 50 km. The outer part of the shelf has uniform salinity distribution of about 17.9. It is connected, on its offshore side, to the Rim Current frontal zone, which is characterized by 18.0±0.1 salinity conforming over the lower topographic slope zone between 1000 m and 2000 m bathymetric contours. A major offshore protrusion of the low salinity inner shelf waters takes place southeastward of the Danube delta, across the topographic slope up to the 2000 m depth contour. We note that this feature emerges as an isolated anticyclonic eddy in the surface dynamic topography map (Fig. 2a) since the dynamic height computations do not include the shelf region with depths shallower than 500 m. A similar feature is also seen in the September 1991 survey (Fig. 5a in Oguz et al. 1994). To the south of this filament, the inner shelf and the Rim Current frontal zones are combined together to form a unified shelf break frontal structure across the steep topographic changes of the region (Fig. 7). To the north of this filament,

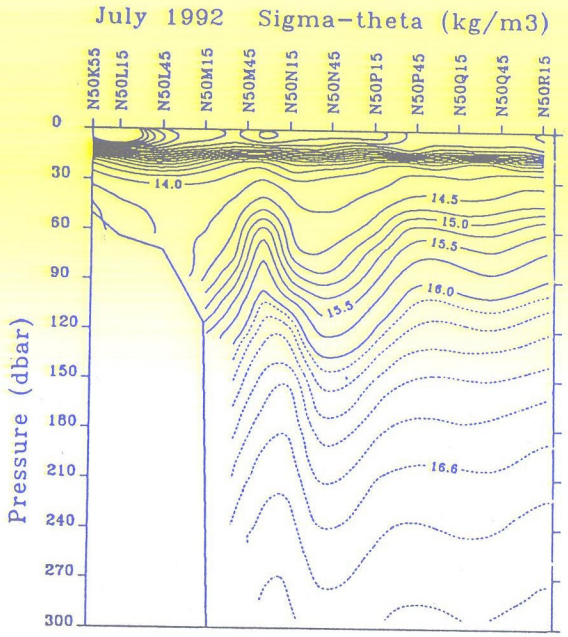

Figure 7. Zonal sigma-t transect across the northwestern shelf, indicated by section D in Fig. 1.

on the other hand, the surface intensified fresh waters with density of about 10 kg/m^3 are marked above the seasonal thermocline-pycnocline near the western coast (Fig. 7). Below the seasonal thermocline, the entire shelf region is characterized by almost horizontally uniform density of ~14.2 kg/m^3 with a bottom-to-surface shelf break density front situated around approximately 100 m depth.

Contrary to small amplitude meanders observed in the dynamic height topography map shown in Fig. 2a or in geostrophic current field given in Fig. 3a, the surface salinity pattern (Fig. 6) exhibits a highly variable, narrow (~25km) frontal zone identified generally by the salinity values between 17.7 and 18.2. The two cyclonic gyres of the interior have spatially uniform salinities of about 18.2-18.3, increasing locally up to 18.5. The areas of lower salinity coastal waters, having typical salinities of 17.2-17.6, coincide with the anticyclonic eddies identified earlier in the surface DHT map. The fresh water influence originated from the northwestern shelf is traced clearly up to the Sakarya Eddy region near the begining of the curved Turkish coastline at 31.5°E. Relatively lower salinity coastal waters of about 17.2 are also present in the Kizilirmak and Yesilirmak River discharge regions along the Turkish coast near 36°E as well as off the

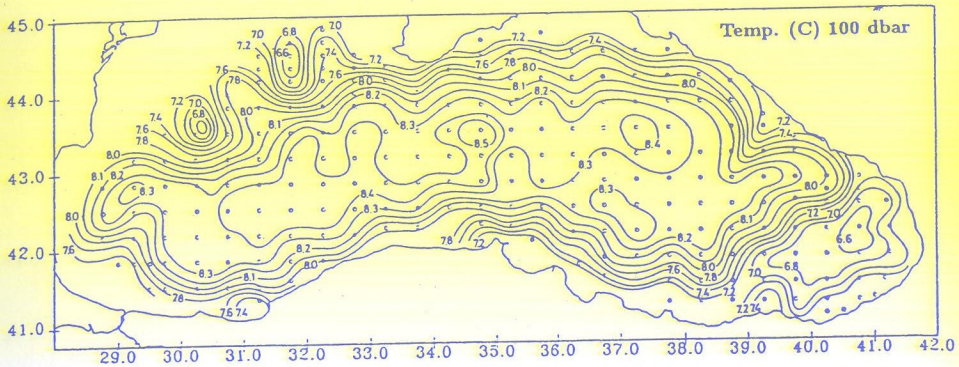

Figure 8a. Potential temperature distribution (°C) at 100 m depth. The contour intervals vary for clarity of presentation.

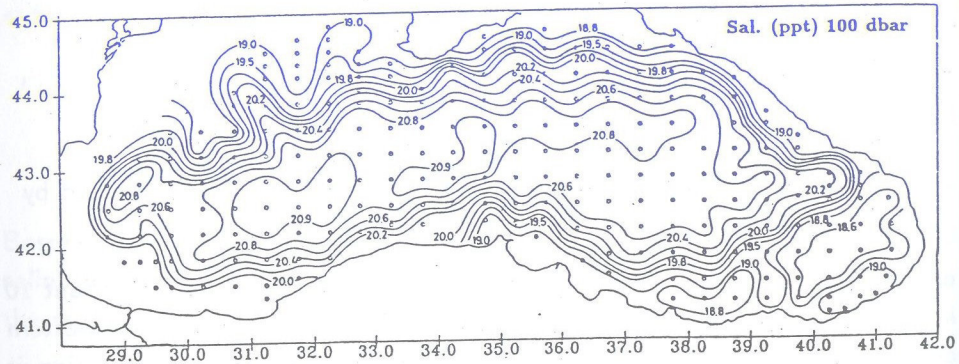

Figure 8b. Salinity distribution at 100 m depth. The contour intervals vary for clarity of presentation.

Sea of Azov on the northern coast.

Comparision of Fig. 6 with Fig. 5a of Oguz et al. (1994) for the September 1991 survey suggests temporal variability in the position of the salinity front between the northwestern shelf and the interior of the western basin depending on the mesoscale structure of the circulation and thermohaline fields. The cross-shelf variability of these frontal structures provide an efficient mechanism for the exchange between the NWS and the deep interior basin.

The temperature and salinity fields at the subsurface levels are in better agreement with the corresponding dynamic height fields. At 100 m depth, the interior basin is characterized by the temperature values of 8.3-8.5 °C (Fig. 8a), signifying the relatively warmer temperatures below the cold intermediate layer. Towards the periphery, temperature decreases gradually up to the values of 7.2 °C near the coast and of 6.6°C within the centers of the anticyclonic eddies. The warmer interior waters of the basin are accompanied with the relatively higher salinity values of about 20.8 ppt, decreasing by about 1.0 ppt towards the coast (Fig. 8b). The frontal salinity variations associated with the Rim Current zone at this depth of the pycnocline region is, therefore, more pronounced as compared with its surface variations.

It is of interest to compare the distributions of the CIL and of the oxic/anoxic interface level in the present survey with those of the September-October 1990 and September 1991 survey described in Oguz et al. (1993a,1994). The lower boundary of the CIL, characterized by the 8 °C temperature surface, is given in Fig. 9a. It is located at about 70 m depth within the basin interior, deepening sharply across the Rim Current frontal zone to the depth of 140 m near the coast. In the Batumi anticyclonic eddy it reaches the depth of 170 m. While the position of the lower CIL boundary in this survey is closely similar to that of the previous surveys (see e.g. Fig. 13a in Oguz et al., 1994), the cross-frontal deepening is much pronounced here, and differs from the September 1991 survey by about 20 m. The topography of the oxic/anoxic interface level defined by the 16.2 kg/m^3 sigma-theta surface is situated at ~100 m depth (Fig. 9b). As compared with the September 1991 survey, it is approximately 10 m elevated and reveals more pronounced lateral variations across the Rim Current frontal zone. The typical coastal depth of the interface position is 160-170 m, increasing to about 200 m within the Batumi eddy.

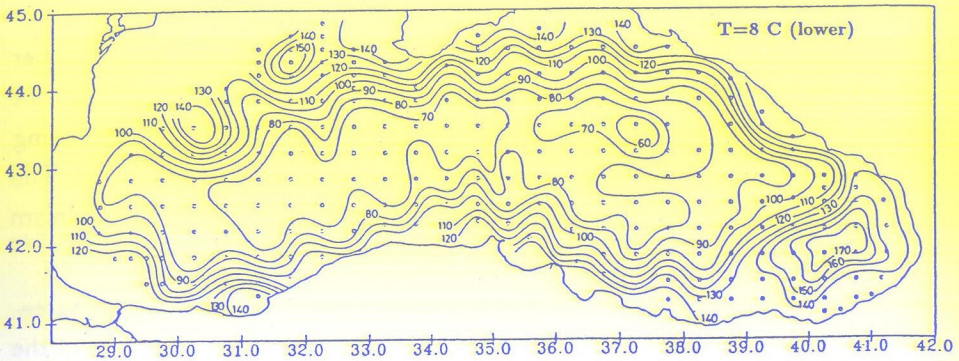

Figure 9a. Topography of the lower boundary of the Cold Intermediate Layer.

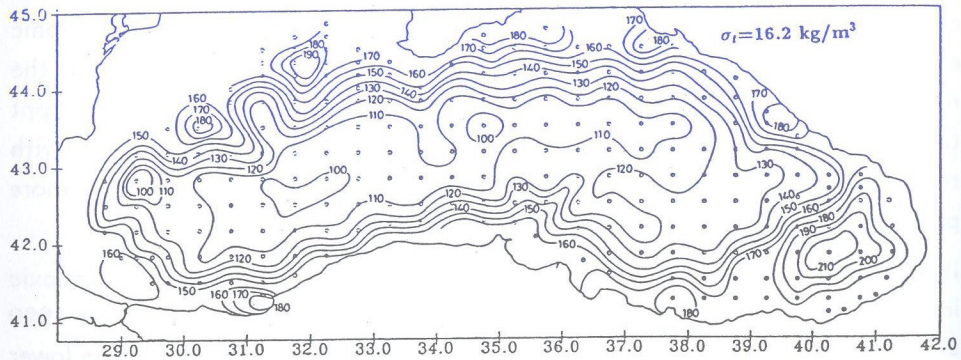

Figure 9b. Topography of 16.2 sigma-t surface, defining the lower boundary of the suboxic zone and begining of the sulphide pool.

5. Summary and Conclusions

A basinwide kinematical description of the circulation and hydrographic characteristics of the Black Sea is presented using findings from the multi-ship quasi-synoptic field survey performed during July 1992. More than 300 stations were visited with a nominal grid spacing of 20 miles with a resolution of approximately twice of the baroclinic Rossby radius of deformation. This survey is the second basin-wide medium resolution survey realized quasi-synoptically within the framework of multi-instutional corporation of the riparian countries.

During summer (July) 1992, the current regime within the Black Sea is dominated by a cyclonic basin-wide cell surrounded by a convoluted peripheral current system and some coastal anticyclonic mesoscale eddies. The interior of the cell consists of two separate cyclonic gyres near the surface, but only one elongated gyre within the rest of the water column below the seasonal thermocline-pycnocline situated approximately at 20m depth. As compared to the baroclinic circulation observed earlier during September 1991, the surface as well as deeper level circulations have generally more uniform interior structure and smoother onshore-offshore variability of the Rim Current. Thus, this survey does not possess intense meanders and offshore filaments as we have seen earlier during September 1991. Many of the coastally-attached anticyclonic eddies given in our upper layer schematic circulation pattern (Oguz et al.,1993a), such as the Sakarya Eddy, Batumi Eddy, Caucasian Eddy, Crimean and Sevastopol Eddies, Kali Akra Eddy, are also present in this survey. In addition, another anticyclonic eddy occupies the central part of the eastern basin at the sub-pycnocline levels below a horizontally quiescent region within the upper layer.

The nature of interaction of northwestern shelf waters with the waters of the Rim Current frontal zone is also distinctly different from that of September 1991 case. In the previous survey, the Rim Current frontal zone was situated roughly over the upper topographic slope near the shelf break and was closer to the fresh water induced inner shelf front. This allowed for considerable interactions between the shelf and interior waters, and shoreward intrusions of interior waters over the relatively smooth and wide topographic slope region. On the other hand, in the present survey, the opposite situation is developed. The Rim Current zone is shifted further offshore and confined to the lower topographic slope. The outer shelf region up to the inner shelf front acts as a

buffer zone between the interior and northwestern shelf waters.

The July 1992 survey also provides an example for short term, transient atmospheric effects on the regional circulation structures. In particular, we note generation of a cold water patch along the Turkish coast near Cape Sinop due to the upwelling favorable wind events. This type of features is noted frequently in satellite imagery for the Black Sea during summer months (Oguz et al.,1992).

When compared with the horizontal salinity distribution, the geostrophic currents computed using the thermal wind balance do not seem to reflect the actual current field consistent with the highly complex salinity and density patterns. This implies important contribution of ageostrophic effects to the flow field neglected in the dynamic height computations. The baroclinic instability mechanism associated with the nonlinear internal dynamics of the flow field seems to be an important process in the evolution of the horizontal circulation fields.

Acknowledgement

This study has been supported by the NATO Science for Stability Program, as well as Academies of Science in Bulgaria, Romania, Ukraine, and the Turkish Scientific and Technical Research Council.

References

[1] Aubrey D.G., T. Oguz, E. Demirov, V. Ivanov, T. McSherry, V. Di- acanu, E. Nikolaenko (1992) HydroBlack'91: Report of the CTD calibration workshop. ComsBlack 92-005 Technical Report. Woods Hole Oceanographic Institution Technical Report WHOI-92-10, CRC-92-OI,126pp.

[2] Aubrey, D., S. Moncheva, E. Demirov, V. Diaconu, A. Dimitrov (1996) Environmental changes in the western Black Sea related to antropogenic and natural conditions. J. Marine Systems, 7, 411-425.

[3] Basturk, O., C. Saydam, I. Salihoglu, L.V. Eremeeva, S.K. Konovalov, A. Stoyanov, A. Dimitrov, A. Cociasu, L. Dorogan, M. Altabet (1994) Vertical variations in the principal cheznical properties of the Black Sea in the autumn of 1991. J. Marine Chem., 45,149-166.

[4] Blatov S.S., N.P. Bulgakov, V.A. Ivanov, A.N. Kosarev, V.S. Tujilkin (1984) Variability of the hydrophysical fields in the Black Sea. Hydrometeoizdat, Leningrad, 249 pp. (In Russian).

[5] Eremeev, V. N., L. M. Ivanov, S. V. Kochergin, O. V. Melnichenko (1992) Seasonal variability and types of currents in the upper layer of the Black Sea. Sov. J. Phys. Oceanogr., 3,193-208.

[6] Konovalov, S., S. Tugrul, O. Basturk, I. Salihoglu (1998) Spatial isopycnal analysis of the main pycnocline chemistry of the Black Sea: Seasonal and interannual variations. to appear in: *NATO ASI Series on the Proceedings of the NATO Advanced Research Workshop "Sensitivity to Change: Black Sea, Baltic Sea and North Sea, E. Ozsoy and A. Mikaelyan (Editors), NATO ASI Series 2, Environment-Vol.27, 455-469.*

[7] Murray, J. W. (1991) Black Sea Oceanography: Results from the 1988 Black Sea Expedition. Deep Sea Research, V. 38, Supplementary Issue No.2A, 1266pp.

[8] Oguz, T., M. A. Latif, H. I. Sur, E. Ozsoy, U. Unluata (1991) On the dynamics of the southern Black Sea. NATO ASI Series: The Black Sea Oceanography. E. Izdar and J. W. Murray (Eds). Kluwer Academic Publishers, p.43-64.

[9] Oguz, T., P. E. La Violette, U. Unluata (1992) The Black Sea circulation: its variability as inferred from hydrographic and satellite observations. J. Geophys. Research., 97, p.I2569-12584.

[10] Oguz, T., V.S. Latun, M.A. Latif, V.V. Vladimirov, H. I. Sur, A.A. Markov, E. Ozsoy, B.B. Kotovshchikov, V.V. Eremeev, U. Unluata (1993a) Circulation in the surface and intermediate layers of the Black Sea. Deep Sea Res. I, 40,159'7-1612.

[11] Oguz, T., S. Besiktepe, O. Basturk, I. salihoglu, D. G. aubrey, A. Balci, E. demirov, V. diacanu, L. Dorogan, M. Duman, L. Ivanov, S. Konovalov, A. stayanov, V. Vladimirov, A. Yilmaz (1993b) CoMSBlack'92A Physical

and Cheznical Intercalibration Workshop. Unesco, Intergovermental Oceanographic Commission, Workshop Report No.

[12] Oguz, T., D.G. Aubrey, V.S. Latun, E. Demirov, L. Koveshnikov, V. Diacanu, H.I. Sur, S. Besiktepe, M. Duman, R. Limeburner, V. Eremeev (1994) "Mesoscale circulation and thermohaline structure of the Black Sea observed during HydroBlack'91. Deep Sea Research I, 41, 603-628.

[13] Oguz,T., P. Malanotte-Rizzoli, D. Aubrey (1995): "Wind and Thermohaline circulation of the Black Sea driven by yearly mean climatological forcing". J. Geophysical Research, 100, 6845-6863.

[14] Oguz, T. and P. Malanotte-Rizzoli (1996) "Seasonal variability of wind and thermohaline driven circulation in the Black Sea: Modeling studies". J. Geophysical Research, 101, 16551-16569.

[15] Rachev, N.H. and E.V. stanev (1997) Eddy processes in semienclosed seas: A case study for the Black Sea. J. Phys. Oceanogr., 27, 1581-1601.

[16] Saydam C., S. Tugrul, 0. Basturk, T. Oguz (1993) Identification of the oxic-anoxic interface by isopycnal surfaces in the Black Sea. Deep Sea Res. I, 40,1405-1412.

[17] Stanev, E.V., V.M. Roussenov,N.H. Rachev, J.V. Staneva (1995) Sea response to atmospheric variability: Model study for the Black Sea. J. Marine Systems, 6,241-267.

[18] Sur, H. I., E. Ozsoy, U. Unluata (1994) Boundary current instabilities, upwelling, shelf mixing and eutrophication processes in the Black Sea. Prog. Oceanogr., 33, 249-302.

[19] Tugrul S., O. Basturk, C. Saydam, A. Yilmaz (1992) Changes in the hydrochemistry of the Black Sea inferred from water density profiles. Nature, 359,137-139.

[20] Vladimirov, V.L., V. I. Mankovsky, M.V. Solovev, A.V. Mishonov (1997) Seasonal and long term variability of the Black Sea optical parameters. to appear in: *NATO ASI Series on the Proceedings of the NATO Advanced Research Workshop "Sensitivity to Change: Black Sea, Baltic Sea and North Sea, E. Ozsoy and A. Mikaelyan (Editors), NATO ASI Series 2, Environment-Vol.27, 455-469.*

[21] Yilmaz, A., O.A. Yunev, V. I. Vedernikov, S.Moncheva, A.S. Bologa, A. Cociasu, D. ediger (1998) Unusual temporal variations in the spatial distribution of chlorophyll-a in the Black Sea during 1990-1996. to appear in: *NATO ASI Series on the Proceedings of the Symposium on the Scientific Results of the NATO TU-Black Sea Project, Crimea-Ukraine, June 15-19, 1997.*